IOPscience iopscience.iop.org

Home Search Collections Journals About Contact us My IOPscience

On the insensitivity of liquid diffusivity measurements to deviations from 1D transport

This article has been downloaded from IOPscience. Please scroll down to see the full text article.

1998 J. Phys.: Condens. Matter 10 7113

(http://iopscience.iop.org/0953-8984/10/32/003)

View the table of contents for this issue, or go to the journal homepage for more

Download details:
IP Address: 171.66.16.209
The article was downloaded on 14/05/2010 at 16:40

Please note that terms and conditions apply.

J. Phys.: Condens. Matter **10** (1998) 7113–7120. Printed in the UK PII: S0953-8984(98)93529-9

On the insensitivity of liquid diffusivity measurements to deviations from 1D transport

Lyle B Jalbert, Franz Rosenberger and R Michael Banish

Center for Microgravity and Materials Research, University of Alabama in Huntsville, Huntsville, Al 35899, USA

Received 22 April 1998

Abstract. In liquid diffusion experiments, the diffusion path can be partially obstructed by bubbles/voids, or oxide layers between the segments of a diffusion couple. In addition, there have been claims of macroscopic manifestations of 'wall effects', i.e. a perceived dependence of the diffusivity D on distance from the container wall over macroscopic dimensions. We have numerically simulated the evolution of the concentration field in a 2D diffusion sample in response to such deviations from 1D transport. We found that, owing to the smoothing of the concentration distribution by radial diffusion, significant deviations from the ideal 1D concentration field occur only in the axial direction. On evaluation of the concentration field for an apparent diffusivity D_a, either by the semi-infinite capillary methodology or by the method of Codastefano *et al* (1977 *Rev. Sci. Instrum.* **48** 1650), we found that local obstructions of the transport path have to be in excess of half the transport path's cross-section to result in $D_a \leqslant 0.95D$. Furthermore, we conclude that the radial concentration gradients found in solidified diffusion samples are no evidence for a 'wall effect' but are likely to indicate convective transport contamination.

1. Introduction

Bubbles or voids in liquid diffusion samples [1, 2] can potentially result in erroneous diffusivity determinations. It may also be difficult to prevent the formation of oxide layers, which represent a barrier in the diffusion path, between the segments of a metallic diffusion couple. Other perturbing phenomena observed in diffusion measurements have been generically assigned to 'wall effects' [3–5]. By analogy with surface and grain boundary diffusion, it is speculated that the diffusivity D varies over macroscopic dimensions from the container wall. However, as pointed out by Nachtrieb [5], irrespective of the possible underlying mechanism, 'It is, of course, not credible that a true wall effect could extend much further than a few atomic diameters from the capillary wall, and a reasonable explanation in terms of an experimental artifact must be sought.'

In the following we will examine to what extent such deviations from 1D transport, whether real or conceived, influence the evolution of the concentration distribution in a diffusion sample. In addition we will evaluate the resulting non-ideal distributions in terms of apparent diffusivities D_a utilizing both the semi-infinite sample methodology [6] and the method of Codastefano *et al* [7].

In the semi-infinite technique [6], the diffusion sample is assumed to be infinite in one direction, i.e. with a diffusion path of length L, the initial thickness h of the diffusant source

0953-8984/98/327113+08$19.50 © 1998 IOP Publishing Ltd

(with uniform concentration C_0) must fulfil the condition $h \ll L$. This condition results in the concentration profile at time t

$$C(x,t) = \frac{C_0}{\sqrt{\pi Dt}} \exp\left(\frac{-x^2}{4Dt}\right). \tag{1}$$

Thus, a plot of $\ln C$ against x^2 produces a straight line with the slope given by $-1/(4Dt)$.

In the Codastefano technique [7], one monitors the solute concentrations against time at the positions $x = L/6$ and $5L/6$. The resulting time traces $C_1(t)$ and $C_2(t)$, respectively, are related to the diffusivity through a straight line fit in the form

$$\ln[C_1(t) - C_2(t)] = \text{constant} - \left(\frac{\pi^2 D}{L^2}\right) t. \tag{2}$$

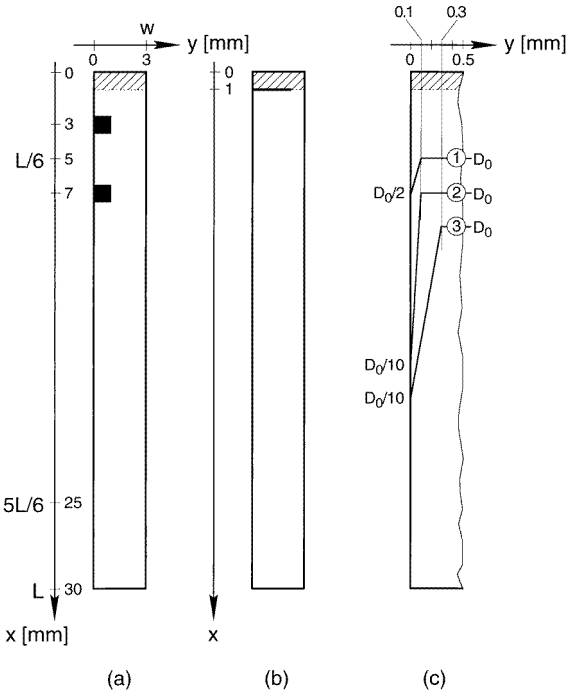

Figure 1. Geometry and modifications of simulation model. Diffusion capillary with (a) voids in liquid, (b) barrier at the source–solvent interface, and (c) y-dependent Ds. Shaded areas indicate regions of initial diffusant concentration C_0.

2. Simulation model

The basic geometry of the 2D simulation model and the various modifications used in the simulations are depicted in figure 1. In accordance with our experimental approach [8], we chose a total sample length $L = 30$, sample width $w = 3$ mm, and initial diffusant layer thickness $h = 1$ mm. Three different sets of conditions resulting in deviations from 1D diffusive transport were assumed. (a) A 1 mm square barrier on one wall, to simulate a void, was centred at $x = 3$ or $x = 7$ mm. Note that these particular positions straddle the Codastefano measurement coordinate $L/6$ at $x = 5$ mm (figure 1(a)). (b) A planar barrier

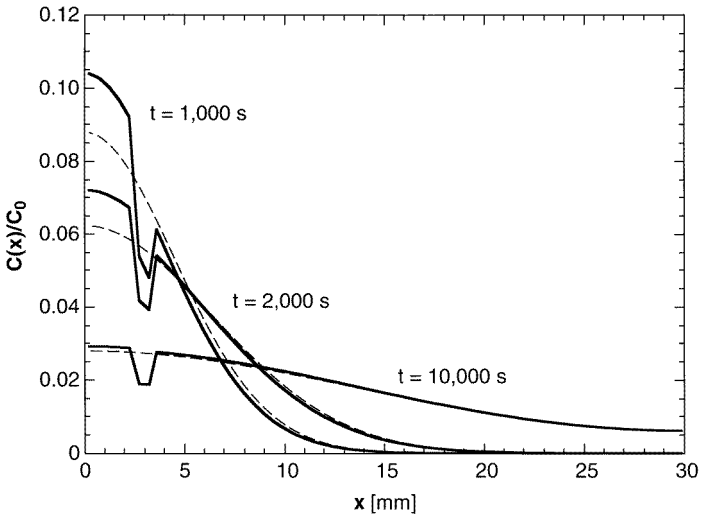

Figure 2. Normalized concentration profiles at three diffusion times. Full curves, with void at $x = 3$ mm; broken curves, unobstructed diffusion.

in the source–solvent interface was extended from one wall to either $y = 0.5$ or $0.75w$ (figure 1(b)). (c) A y-dependent diffusivity was assumed, with either $D = 0.5$ of the input diffusivity D_0 at the wall and then a linear rise to D_0 at $y = 100$ μm, or $D = 10^{-1}D_0$ at the wall rising to D_0 at either 100 or 300 μm; see the schematic D-profiles 1–3 in figure 1(c). The value of 100 μm represents the range at which a change attributed to the 'wall effect' was determined in [6]. The distance $y = 300$ μm corresponds to the sample depth from which 24 keV photons are received in our self-diffusivity measurements with indium [8].

Since isothermal self-diffusion was assumed, the fluid density is uniform throughout the diffusion process. Hence, solutions of the 2D diffusion equation

$$\frac{\partial C}{\partial t} = \frac{\partial}{\partial x_i}\left(D\frac{\partial C}{\partial x_i}\right) \tag{3}$$

where C is the solute mass concentration and $i = 1, 2$, fully describe transport in this case. We used $D_0 = 10.22 \times 10^{-5}$ cm^2 s^{-1} in all our numerical simulations, which corresponds to the self-diffusivity of indium at 900 °C [9].

The numerical simulations were performed with Adaptive Research's CFD 2000 finite volume code, version 3.03. In the void and barrier cases a non-uniform grid of 62×30 and 61×40, respectively, was used. For the wall investigations only half the cell ($0 \leqslant y \leqslant 1.5$ mm) was modelled, utilizing a 100×61 grid. Doubling of the grid number in the x- and y-direction in both the $y = 3$ mm void and 75% barrier cases (the cases with largest concentration gradients) resulted in insignificant changes in the concentration field. All cases were run for 10 000 s to obtain sufficient diffusant concentrations at the $5L/6$ position. For comparison with pure 1D diffusion an unobstructed, uniform-diffusivity run was performed with each grid.

Diffusivities are typically deduced from the total amount of diffusant contained in cross-sectional slices of the sample. Correspondingly, we base our evaluations of the apparent diffusivity D_a in the various cases on axial profiles of the concentration summed across y,

i.e. on

$$C(x,t) = \sum_{y=0}^{w} C(x,y,t). \tag{4}$$

Evaluations using the semi-infinite sample methodology were based on the $C(x,t)$-profile obtained at $t = 2000$ s, at which time the solute barely reaches L. The Codastefano *et al* methodology was applied to the $C(L/6,t)$ and $C(5L/6,t)$ traces obtained, depending on the case, between 3000–5000 and 10 000 s with samples taken every 10 s.

3. Results and discussion

Figure 2 shows $C(x)$-profiles obtained in the case with a void at $x = 3$ mm at three diffusion times. For comparison, we have also plotted the profiles resulting at these times in the 1D diffusion (void-free) case. Both sets of profiles were normalized with respect to C_0. We see that the presence of the void, which blocks one third of the sample cross-section, significantly retards the diffusive spreading of the solute. This is further illustrated by the isoconcentration lines in the upper end of the sample displayed for $t = 1000$ s in figure 3. Note that, as a result of radial diffusion the isoconcentration lines become essentially straight and normal to the x-axis within a short distance downstream from the transport-obstructing void.

Table 1. Apparent diffusivities (10^{-5} cm^2 s^{-1}) obtained in void configurations.

	1D transport	Void @ 3 mm	Void @ 7 mm
Semi-infinite method	10.44 ± 0.174	10.18 ± 0.72	10.17 ± 0.80
Codastefano method	10.2000 ± 0.0001	10.240 ± 0.001	9.9800 ± 0.0005

Table 1 displays the D_a-values obtained for the two void cases and the 1D results, together with respective standard deviations associated with the fits. Interestingly, the 1D transport run, evaluated with the semi-infinite approach, yielded a slightly elevated diffusivity compared with the input $D_0 = 10.22 \times 10^{-5}$ cm^2 s^{-1}. This is not surprizing since the initial source thickness, $h = 1$ mm, only poorly fulfills the required $h \ll L$ condition. Note that all void cases result in D_a-values that are within a few per cent of D_0. Hence, errors introduced by the presence of these voids remain below the experimental resolution, which is of order 5% [8, 10, 11].

Furthermore, table 1 shows that the location of the void has different effects on the apparent diffusivities calculated from the two methods. The semi-infinite sample technique is affected equally regardless of void location while the Codastefano method shows an increase/decrease in D_a with the void upstream/downstream of the $L/6$ measurement location. This, plus the drastically lower standard deviation of the second methodology indicated in tables 1–3, results from the different nature of the input data. The first fitting procedure utilized the $C(x)$-profile that (a) is locally strongly deformed by the void, and (b) is based on a finite resolution grid with 62 points. The Codastefano method, on the other hand, benefits from (a) the smooth variation of $C(x)$ at the two sampling locations ($L/6$ and $5L/6$, i.e. $x = 5$ and 25 in figure 2), and (b) the of O(500) data points used in the fit.

Figure 4 shows the axial profiles $C(x)/C_0$ obtained with the 75% barrier (figure 1(b)) at three diffusion times together with the corresponding profiles resulting on the same grid from the unobstructed 1D diffusion case. One sees that this barrier causes a pronounced

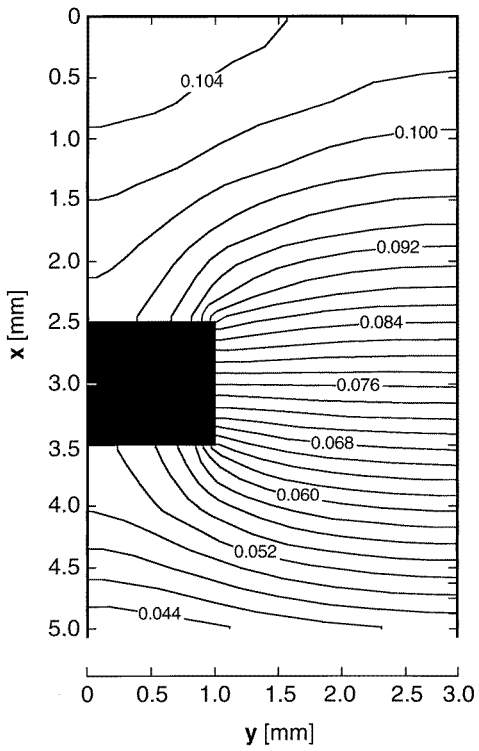

Figure 3. Normalized isoconcentration lines $C(x, y)/C_0$ in the upper part of the capillary at $t = 1000$ s with void at $x = 3$ mm.

Table 2. Apparent diffusivities (10^{-5} cm^2 s^{-1}) obtained in barrier configurations.

	1D transport	50% barrier	75% barrier
Semi-infinite method	10.45 ± 0.19	10.05 ± 0.42	9.59 ± 0.90
Codastefano method	10.2000 ± 0.0002	10.1600 ± 0.0004	10.050 ± 0.002

Table 3. Apparent diffusivities (10^{-5} cm^2 s^{-1}) obtained with 'wall effects'.

	1D transport	$D(y)$ case 1	$D(y)$ case 2	$D(y)$ case 3
Semi-infinite method	10.46 ± 0.19	10.29 ± 0.19	10.15 ± 0.19	9.55 ± 0.20
Codastefano method	10.1900 ± 0.0002	10.0400 ± 0.0002	9.9000 ± 0.0002	9.3000 ± 0.0003

retention of the solute in the region of initial diffusant location. However, table 2 reveals that even in this drastic case, the error in the deduced diffusivities is barely larger than the above typical experimental uncertainties. Here again the semi-infinite method is somewhat more sensitive than the Codastefano method.

The results of the various assumed 'wall effects' are summarized in table 3. Even with the particularly unphysical assumption of case 3, D_a-values are obtained that lie within the uncertainty of many measurements.

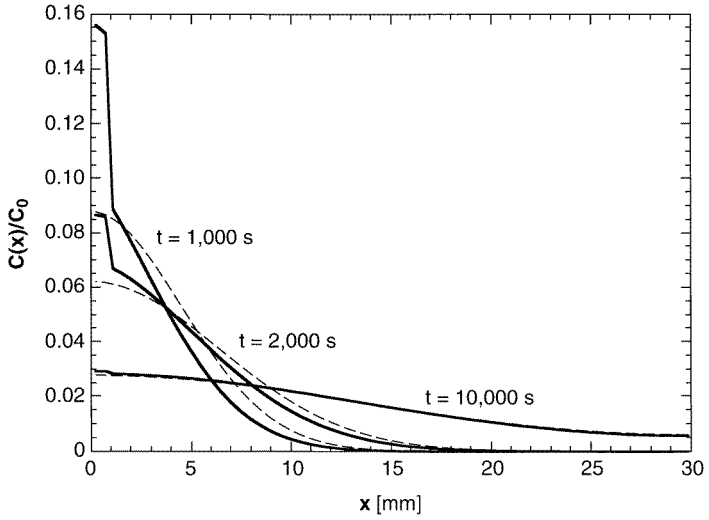

Figure 4. Normalized concentration profiles at three diffusion times. Full curves, with 75% barrier at $x = 1$ mm; broken curves, unobstructed diffusion.

Table 4. Maximum normalized radial concentration variation at $x = L/6$.

Case	Radial $\Delta C/C$ (%)	Time of occurrence (s)
$D(y)$ case 1	0.014	250
$D(y)$ case 2	0.028	230
$D(y)$ case 3	0.082	230

The insensitivity of the concentration distribution to postulated 'wall effects' is further illustrated in figure 5, in which we have plotted the concentration difference (normalized to the samples maximum C) between case 3 and the 1D transport result at 300 s. It is evident that solute redistribution by radial diffusion prevents the formation of significant concentration gradients across the width of the sample. This is also supported by the low values of the maximum radial concentration variation at position $x = L/6$ listed in table 4.

Note that these maxima occur early in the diffusion runs. Thus they are unlikely to be detectable in diffusivity measurements. As a consequence, experimental findings of radial concentration gradients in cylindrical diffusion samples indicate convective contamination (for detailed examples see [12]) rather than inferred dependences of diffusivity on the distance from the container wall.

4. Conclusions

The above 2D simulations show that the influence of the model voids, barriers and 'wall effects' on concentration distributions in diffusion samples and the subsequently deduced diffusivities is rather marginal. Note that in real, 3D systems, owing to the lower cross-sectional fraction taken on by such obstacles of the same radial dimensions, the deviations from unobstructed diffusive transport will be even less significant. Hence, we conclude that the contamination of diffusivity measurements owing to such geometrical parameters will in

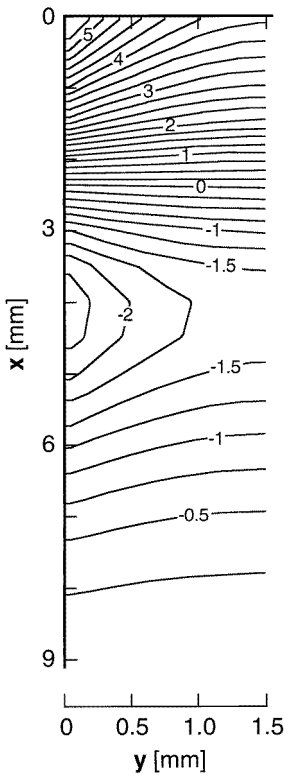

Figure 5. Difference in concentration between the 'wall effect' case 3 and uniform diffusion, $\Delta C(x, y)$, normalized to the maximum concentration, obtained in the top part of the sample at $t = 300$ s. Numbers in 10^{-2}%.

most cases be negligible compared with the convective contamination arising from sample non-isothermality [12].

Acknowledgments

This research has been supported by the National Aeronautics and Space Administration under contract NCC8-99, and by the State of Alabama through the Center for Microgravity and Materials Research at the University of Alabama in Huntsville. We are much obliged to J I D Alexander for advice on the use of the CFD code.

References

[1] Pollman K W, Stodieck L S and Luttges M W 1994 *Microgravity Sci. Tech.* **7** 50
[2] Weinberg F and Mui C 1994 *Can. Metal. Quart.* **33** 233
[3] Careri G, Paoletti A and Vincentini M 1958 *Nuovo Cimento* **10** 1088
[4] Foster J P and Reynik R J 1973 *Met. Trans.* **4** 207
[5] Nachtrieb N H 1967 *Proc. Int. Conf. on Properties in Liquid Metals* ed P D Adams, H A Davies and S G Epstein (London: Taylor and Francis) p 309
[6] Crank J 1956 *The Mathematics of Diffusion* (Oxford: Clarendon)
[7] Codastefano P, Di Russo A and Zanza V 1977 *Rev. Sci. Instrum.* **48** 1650

[8] Jalbert L B, Banish R M and Rosenberger F 1998 *Phys. Rev.* E **57** 1727
[9] Lodding V A 1956 *Z. Naturf.* a **11** 200
[10] Nachtrieb N H 1976 *Berichte Bunsenges.* **80** 678
[11] Simoji M and Itami T 1986 *Atomic Transport in Liquid Metals* (Aedermansdorf, Switzerland: Trans. Tech.)
[12] Alexander J I D, Ramus J-F and Rosenberger F 1996 *Microgravity Sci. Tech.* **9** 158